JNeurosci
THE JOURNAL OF NEUROSCIENCE

Research Articles: Behavioral/Cognitive

The Lifespan Trajectory of the Encoding-Retrieval flip. A Multi-modal Examination of Medial Parietal Cortex Contributions to Episodic Memory

Inge K. Amlien[1], Markus Sneve[1], Didac Vidal-Piñeiro[1], Kristine B. Walhovd[1,2] and Anders M. Fjell[1,2]

[1]*Centre for Lifespan Changes in Brain and Cognition, University of Oslo, Norway*
[2]*Department of Radiology and Nuclear Medicine, Oslo University Hospital, Oslo, Norway*

DOI: 10.1523/JNEUROSCI.1702-17.2018

Received: 19 June 2017

Revised: 21 June 2018

Accepted: 23 June 2018

Published: 24 August 2018

Author contributions: I.K.A., M.H.S., D.V.-P., K.W., and A.M.F. designed research; I.K.A., M.H.S., and D.V.-P. performed research; I.K.A., M.H.S., D.V.-P., K.W., and A.M.F. analyzed data; I.K.A. wrote the first draft of the paper; I.K.A., M.H.S., D.V.-P., K.W., and A.M.F. wrote the paper.

Conflict of Interest: The authors declare no competing financial interests.

The project has received funding from the European Research Council's Starting Grant scheme under grant agreements 283634, 725025 (to AMF) and 313440 (to KBW), and was also supported by grants from the Norwegian Research Council and by the Department of Psychology, University of Oslo. Data processing was performed on the TSD (Tjeneste for Sensitive Data) facilities, owned by the University of Oslo, operated and developed by the TSD service group at the University of Oslo, IT-Department (USIT).

Address correspondence to: Inge K Amlien, Dept of Psychology, Pb. 1094 Blindern, 0317 Oslo, Norway, phone: +47 22 84 50 00, fax: +47 22 84 50 01, e-mail: inge.amlien@psykologi.uio.no

Cite as: J. Neurosci ; 10.1523/JNEUROSCI.1702-17.2018

The Lifespan Trajectory of the Encoding-Retrieval flip. A Multi-modal Examination of Medial Parietal Cortex Contributions to Episodic Memory

Running title: E/R flip development

Inge K. Amlien[1*], Markus Sneve[1], Didac Vidal-Piñeiro[1], Kristine B. Walhovd[1,2], Anders M. Fjell[1,2]

[1] Centre for Lifespan Changes in Brain and Cognition, University of Oslo, Norway

[2] Department of Radiology and Nuclear Medicine, Oslo University Hospital, Oslo, Norway

* Address correspondence to: Inge K Amlien, Dept of Psychology, Pb. 1094 Blindern, 0317 Oslo, Norway, phone: +47 22 84 50 00, fax: +47 22 84 50 01, e-mail: inge.amlien@psykologi.uio.no

Number of pages: 47 Number of figures: 12 Number of tables: 4

Number of words in Abstract: 241

Number of words in Introduction: 644

Number of words in Discussion: 1500

Acknowledgements

The project has received funding from the European Research Council's Starting Grant scheme under grant agreements 283634, 725025 (to AMF) and 313440 (to KBW), and was also supported by grants from the Norwegian Research Council and by the Department of Psychology, University of Oslo. Data processing was performed on the TSD (Tjeneste for Sensitive Data) facilities, owned by the University of Oslo, operated and developed by the TSD service group at the University of Oslo, IT-Department (USIT).

Conflicts of interest

The authors declare no competing financial interests.

Abstract

The formation of episodic memories is associated with deactivation during encoding and activation during retrieval in the posteromedial cortices (PMC). We hypothesized that the encoding-retrieval flip (E/R flip) is a critical component of episodic memory across the life span, as structural and metabolic changes in the PMC coincide with the fine tuning of the episodic memory system in development and the reductions of memory performance in aging. The aims of the present study were first to describe life-span trajectories of PMC encoding and retrieval activity in 270 human participants (167 females) from 6-80 years. Second, to construct a model for episodic memory development, where contributions from brain activity, cortical thickness, and structural connectivity are accounted for. We found that modulation of neural activity in response to memory encoding and retrieval demands was not fully developed until adolescence, and decreased from adulthood. The magnitude of the E/R flip was related to source memory, and 55 % of the age-related variance in source memory performance during childhood and adolescence could be accounted for by the E/R flip, cortical thickness and mean diffusivity together. However, only cortical thickness and the E/R flip provided unique contributions to explain memory performance. The results suggest that neural dynamics in the PMC is related to the development of episodic memory during childhood and adolescence. The similar trajectories of the E/R flip and episodic memory emergence and decline through development and aging further suggests that a life-long relationship exists.

Significance statement

Modulation of neural activity in the posteromedial cortices (PMC) in response to memory encoding and retrieval demands (E/R flip) does not reach its peak until adolescence, and decreases from adulthood through old age. The magnitude of the E/R flip is related to source memory, and 55% of the age-related variance in source memory performance during childhood and adolescence can be accounted for by the E/R flip and brain structure together. The results suggest that neural dynamics in the PMC is related to the development of episodic memory function during childhood and adolescence, and the similar trajectories of the E/R flip and episodic memory performance, through development and aging, suggests that a life-long relationship exists.

Introduction

The posteromedial cortex (PMC) deactivates during successful episodic memory encoding (Daselaar et al., 2004) and activates during successful retrieval (Wagner et al., 2005; Daselaar et al., 2009a). This reversal of functional response is likely critical for memory and has been dubbed the encoding/retrieval flip (E/R flip) (Vannini et al., 2010; Huijbers et al., 2012; 2013; Gilmore et al., 2015). Interestingly, PMC is among the regions that undergo the most rapid structural (Brown and Jernigan, 2012; Tamnes et al., 2013; Amlien et al., 2016) and metabolic (Blüml et al., 2013; Degnan et al., 2014) changes during late childhood and adolescence, coinciding with episodic memory development (Ofen et al., 2007; Ghetti and Bunge, 2012). An intriguing question is whether improvement in the ability to dynamically regulate PMC activity during encoding and retrieval can account for developmental gains in memory. The aims of the present study were first to test life-span trajectories of PMC encoding and retrieval activity, and then to construct a model for episodic memory development where the contributions from brain activity patterns, cortical thickness (CT), and structural connectivity are accounted for.

PMC encoding deactivation and retrieval activation for remembered items was first reported more than 15 years ago (Otten and Rugg, 2001; Wagner and Davachi, 2001; Lundstrom et al., 2003; Daselaar et al., 2004; Wagner et al., 2005; Daselaar et al., 2009a; Duarte et al., 2010), see Kim (2011; 2013) for reviews. Studies examining the E/R flip directly are few (Vannini et al., 2010; W Huijbers, 2012; Gilmore et al., 2015), and we are aware of one study examining the E/R flip in aging (Vannini et al., 2013), showing that the magnitude of functional modulation in PMC declines with age and is related to memory performance.

While the role of the PMC in memory and the mechanisms behind the E/R flip are not fully understood, the function of the PMC is often linked to the default mode network (DMN). The DMN may support mental processes that are inwardly oriented and occur spontaneously during rest. The network deactivates when attention is directed towards external stimuli or during an active task (Raichle et al., 2001; Buckner et al., 2008). Deactivation of PMC during encoding may thus be interpreted as a result of attending to external stimuli and actively encoding information. Increased retrieval activation may on the other hand reflect the process of orienting towards internal representations of stored memories. The DMN has been identified in infants (Gao, 2009), but the organization of functional connectivity in the brain still undergoes changes during development (Supekar et al., 2009; Power et al., 2010). Deactivation of the PMC during episodic memory encoding is less pronounced in children than in adults. It is however unknown whether the lack of disengagement reflects reduced functional modulation, or if children show the same range of modulation between encoding and retrieval as adults, with less deactivation, but increased activation during retrieval (Chai et al., 2014).

In the present study, we tested patterns of functional modulation of activity in the PMC between encoding and retrieval of episodic memories during development and aging, in participants from 6 to 80 years old. We hypothesized a protracted development of modulation of PMC activity evidenced by an increased E/R flip, with subsequent reductions in aging, causing children and older adults to show similar PMC activity patterns. Further, we hypothesized that CT and structural connectivity both would be positively related to the magnitude of the E/R flip and source memory performance in childhood and adolescence, and that a multi-modal model would explain a substantial amount of the age-related variance in source memory development. An extended sample (6-80 years) was used to describe the

lifespan trajectories of the E/R flip and the question of whether the pattern seen in children mirrors the reductions reported in aging, while the multi-modal analyses were restricted to the developmental subsample with complete multi-modal data (6-30 years).

Materials and Methods

Participants

The full sample included in the analyses counted 270 participants from 6 to 80 years. The participant pool consisted of newly recruited participants, as well as participants recruited from existing studies coordinated from the Center for Lifespan Changes in Brain and Cognition (LCBC) at the Department of Psychology, University of Oslo, Norway (The Norwegian Mother and Child Cohort Neurocognitive Study (MOBA)/ Neurocognitive Development/ Cognition and Plasticity Through the Life-span). The research project was approved by the Regional Ethical Committee of South Norway, and all participants age > 12 gave written informed consent, while participants age < 12 gave oral informed consent to participate in the study. For all participants aged < 18, written informed consent was also obtained from their guardians. The participants had no history of neurological or psychiatric disorders, chronic illness, learning disabilities, or use of medicines known to affect nervous system functioning. They were also right-handed, spoke Norwegian fluently and had normal or corrected to normal hearing and vision. All participants were rewarded for their participation with cash or gift cards, and the 13 participants recruited through the MOBA study also with gifts (toys). 340 participants were considered for inclusion in the study. 38 participants were selected for a delayed memory test, and were thus excluded from the full sample. 11 participants were excluded because of various problems during MR-acquisition leading to invalid or un-analyzable data (relative movement during fMRI exceeding 1.5 mm, missing trials, sound problems during task, operator error during scan, etc.), 15 were excluded because they remembered less than 10 % of the items with source memory, or had more than 50 % false alarms or misses. 5 participants were excluded for neuroactive medication or alcohol intake, and one participant was excluded because of incidental MR-findings on the

radiological exam. After exclusions, the developmental subsample consisted of 105 participants eligible for fMRI analyses with ages ranging from 6 to 30 years (*M* = 19.45, SD = 5.72, 61 females), out of which 90 participants had the full set of data and were included in the multimodal and SEM analyses. The sample of healthy older participants consisted of 165 participants, aged 30-80 years (*M* = 55.80, SD = 12.27, 106 females). The full sample entered in the analyses thus consisted of 270 participants (*M* = 41.66, SD = 20.48, females = 167) who had undergone the complete MR-scanning procedure. Task-fMRI data from 72 of the young and 143 of the older participants have previously been used in studies with non-overlapping research questions (Sneve et al., 2015; Vidal-Piñeiro et al., 2017).

Memory task and procedure

The participants were scanned using fMRI during both encoding and retrieval while performing an incidental memory task (Sneve et al., 2015). The stimulus material for the memory task consisted of 100 line drawings depicting common objects, accompanied by one of two questions asking if the participants could either lift or eat the object. The item-question-combinations (ICQs) were locked, in such a fashion that all objects had one specific question associated with it. For example, the drawing of a wheelchair always had the question "Can you eat it?" associated with it. During the encoding phase, two runs with 50 objects each were presented for the participants. Each run started with a period of 11s recording baseline activity, during which a fixation cross was presented. This baseline activity recording was also repeated in the middle and at the end of each run. Every encoding trial started with a recorded female voice asking the participant the Norwegian equivalent of one of two questions: "Can you lift it?" or "Can you eat it?". One second after the question onset, a line drawing appeared on screen. The participant responded to the question by pressing a button with the index finger on either the left or right response grip, according to instructions on

screen. The hand used to produce a “yes” response was counterbalanced between participants. After a response window of two seconds, the line drawing was replaced by a fixation cross which remained on screen during the interstimulus interval (ITI), which varied randomly between 1-7 seconds with an exponential distribution over 4 discrete intervals (mean duration 2.98 s SD=2.49s). The jittering of stimulus onsets facilitated later disentangling of fMRI data reflecting different encoding conditions (Ollinger et al., 2001; Serences, 2004).

When the encoding session was over, the participants were taken out of the scanner, and were seated in a waiting area for about 1 hour until the next scan session. The participants were not explicitly instructed to remember the stimuli, and were not informed of the memory test until just before the first test trial. The test runs were also performed during fMRI in the same scanner. Test trials started with the pre-recorded female voice asking (question 1): “Have you seen this before?” A picture of the item then appeared on screen, and the participant responded by pressing the response grip button corresponding to “yes” or “no”. If the participant responded “no” or did not respond within two seconds, the current trial was aborted and the experiment continued with the next trial. If the participant answered “yes (I have seen this item before)”, a follow-up question was presented (question 2): “Do you remember what you were supposed to do with it?” Again, if the participant answered “no”, the current trial was aborted, and the experiment proceeded with the next trial. If the participant answered that (s)he remembered what (s)he was supposed to do with the item, a follow-up question was presented (question 3): “What were you supposed to do with it?” Here, the participant was given a two-alternative forced choice between the actions presented during the encoding phase. For statistical analyses, test trial responses were classified as follows: (1) recognition (correct “yes” response to question 1), (2) source memory (correct “yes” response to question 1 and 2 and correct response to question 3); or (3) miss (incorrect

185 “no” response to question 1). Note that the specific questions asked during scanning were
186 simplified to fit within the temporal limits of the paradigm, but that all participants were
187 instructed in detail before the test session that the questions pertained to the item-action
188 evaluation performed at encoding.

189 All visual stimuli (~10 visual degrees in diameter) were presented on an NNL 32’’ LCD
190 Monitor at a resolution of 1920 × 1080 pixels (NordicNeuroLab, Bergen, Norway), positioned
191 176 cm from the mirror attached to the coil. Participants responded using the ResponseGrip
192 system (NordicNeuroLab, Bergen, Norway) and were shown a response feedback indicator on
193 the screen. Auditory stimuli were presented to the participants through headphones.

194 MRI data acquisition

195 *fMRI*

196 A 3T Siemens Skyra system (Siemens Medical Systems, Erlangen, Germany) with a 24-
197 channel Siemens head coil was used to acquire all MR images during the memory task. Two
198 fMRI runs were acquired during encoding, and four were acquired during retrieval, all with
199 the same parameters: 43 transversally oriented gapless slices were recorded using a BOLD-
200 sensitive T2*-weighted echo planar image (EPI) sequence (repetition time (TR) = 2390 ms,
201 echo time (TE) = 30 ms, flip angle = 90°, voxel size = 3×3×3mm, field of view (FOV) = 224
202 × 224 mm, interleaved acquisition (GRAPPA acceleration factor = 2). Three dummy volumes
203 were collected at the start of each run, to avoid T1 saturation effects in the analyzed data.
204 Each encoding run consisted of 131 volumes, while the length of the retrieval runs varied
205 dependent on the participants’ responses, as negative answers to any of the first two questions
206 ended the trial. A standard double-echo gradient-echo field map sequence was acquired for
207 distortion correction of the EPI images.

208 ***Diffusion tensor imaging***

209 A single-shot twice-refocused spin-echo echo planar imaging (EPI) with 64 directions was
210 acquired with the following parameters: TR = 9300 ms, TE = 87 ms, b-value = 1000 s/mm^2,
211 voxel size = 2.0 × 2.0 × 2.0 mm, slice spacing = 2.6 mm, FOV = 256, matrix size = 128 × 130
212 × 70, 1 non-diffusion-weighted (b = 0) image. In order to correct for eddy current-induced
213 image distortions, 1 b0-weighted image was acquired with the reverse phase encoding, but
214 otherwise identical acquisition parameters. These images were obtained on the same 3T
215 magnet as the fMRI images. The participants recruited through MOBA already had recorded
216 DTI scans with 32 directions acquired on a 1.5 T Siemens Avanto scanner (Siemens Medical
217 Solutions) using a 12-channel head coil with the following parameters: TR = 8200 ms,
218 TE = 81 ms, b-value = 700 s/mm^{2,} voxel size = 2.0 x 2.0 x 2.0 mm, field of view = 128,
219 matrix size = 128 × 128 × 64, number of b0 images = 5, GRAPPA acceleration factor = 2.
220 One adolescent and four adults did not have adequate DTI images, and were thus excluded
221 from the DTI analyses.

222 ***sMRI***

223 One sagittal T1-weighted MPRAGE volume consisting of 176 sagittally oriented slices was
224 obtained using a turbo field echo pulse sequence (TR = 2300 ms, TE = 2.98 ms, flip angle =
225 8°, voxel size = 1 × 1 × 1 mm, FOV = 256 × 256 mm). For the youngest children, integrated
226 parallel acquisition techniques (iPAT) was used, acquiring multiple T1 scans within a short
227 scan time, enabling us to discard scans with residual movement and average the scans with
228 sufficient quality. Previous studies have shown that accelerated imaging does not introduce
229 measurement bias in surface-based measures when using FreeSurfer for image analysis,
230 compared with a standard MPRAGE protocol with otherwise identical voxel dimensions and
231 sequence parameters (Wonderlick et al., 2009), which is in accordance with our own analyses.

232 Several other MRI volumes were recorded during the session, not related to the current
233 experiment, including sequences intended for and examined by a radiologist to rule out and
234 medically follow-up any neuroradiological findings in the sample. Total scanning times were
235 approximately 58 minutes for the encoding session, and 45 minutes for the retrieval session,
236 depending on the participants' responses. The youngest children in the MOBA sample spent
237 less time in the scanner during the encoding (~ 25 min) and retrieval (~45 min) fMRI tasks, as
238 the non-task based MRI sequences were recorded in a separate session. The DTI images for
239 these eight participants were collected on average 100.62 days in advance of the fMRI
240 session.

241 Image analysis

242 *fMRI preprocessing*

243 Preprocessing of the functional image data was performed using a combination of the
244 FreeSurfer 5.3 Functional Analysis Stream tools (http://freesurfer.net/fswiki/FsFast) and
245 components from the FSL toolbox (http://fsl.fmrib.ox.ac.uk/fsl/). All functional images were
246 first corrected for distortions caused by b0 inhomogenities in EPI scans (FSL
247 PRELUDE/FUGUE; http://fsl.fmrib.ox.ac.uk/fsl), before the images were motion corrected,
248 slice timing corrected to the middle of a volume's TR, intensity normalized, and registered to
249 the same participants' anatomical volumes using FSL's fMRI Expert Analysis Tools (FEAT).

250 As both children and elderly participants who typically exhibit more head motion during
251 scanning were included in the study, care was taken to address head motion. Relative frame
252 wise displacement estimated by MCFLIRT, averaged across all included participants and runs
253 was .081 mm. The motion distribution followed a U-shaped trajectory relative to age, with the
254 expected pattern of increased relative motion at the extremes of the age range (Figure1).

255 [Insert Figure 1 here]

256 We used a machine learning approach, FMRIB's ICA-based X-noiseifier (FIX), to clean
257 motion-related noise and other artifacts from the fMRI data using a trained multi-level
258 hierarchical classifier (Griffanti et al., 2014; Salimi-Khorshidi et al., 2014). This approach
259 consists of several steps: First the preprocessed data was decomposed into multiple
260 components using MELODIC (Beckmann and Smith, 2004). We then manually classified the
261 components for a subset of the participants (16), and labeled each component as signal or
262 noise. A set of over 180 temporal and spatial features was extracted, and the classifier (an
263 ensemble learning classifier combining k-NN, decision trees and support vector machines)
264 was trained on the manually labeled data set. This enabling learning of the relevant spatial and
265 temporal features needed for building a robust model. We tested the performance of the model
266 on our training data by performing leave-one-out accuracy tests with varying thresholds
267 (Table 1). We set the threshold at a conservative 5, where 10 out of the 16 participants in the
268 training set had 100% true positive rate in the leave-one-out tests. When we examined the
269 discrepancies between the manually labeled components and the components automatically
270 labeled by FIX, we found discrepancies only in the high numbered ICA components, meaning
271 the discrepancies were present only in components explaining miniscule amounts of the
272 variance in the data. The classifier was applied on the complete data set with the selected
273 threshold, and the noise-components (40% average) were regressed from the preprocessed
274 data in addition to 24 motion confound regressors (high pass filtered at 100s).
275 *[Insert Table 1 around here]*
276
277 Before further fMRI analyses commenced, the 4D functional data sets were resampled to a
278 common template ('fsaverage') using the surface-based inter-participant registrations created

during the previous cortical reconstruction.

fMRI analyses

A first-level general linear model (GLM) was set up for each run, consisting of 3 main regressors of interest during encoding (source memory, recognition, miss) + 1 regressor of no interest (trials without a response). 5 main regressor of interest during retrieval (source memory, recognition, miss, correct rejection, false Alarm) + 3 regressors of no interest (no response to question 1, no response to question 2, no response to question 3). The regressors were modelled as events with onsets and durations corresponding to the item presentation period (2s), and convolved with a two-gamma canonical hemodynamic response function (HRF). In addition to the task-regressors and their temporal derivatives, estimated motion correction parameters and a set of polynomials (up to the second degree) were included in the GLM as nuisance regressors. The model and the data were processed through a high-pass filter with a cutoff at 0.01 Hz. Temporal autocorrelations (AR(1)) in the residuals were corrected using a pre-whitening approach.

Parameter estimates for the contrast between fMRI activity of items that were subsequently remembered with full source information vs. implicit baseline fMRI activity, and full source memory vs. misses were calculated for each participant and brought to the group-level, both for activity during encoding, and during retrieval. Statistical significance was tested at each vertex on the cortical surface using GLMs and a weighted least squares approach, treating participants as random effects and weighting them by the inverse of their first-level noise variance (Thirion et al., 2007). Group statistical maps were FDR corrected at $p < .05$.

300 ***Defining the E/R flip ROI***

301 The E/R flip has been defined as the conjunction between successful encoding/retrieval
302 activity contrasted with baseline activity (Vannini et al., 2013), but has also been defined by
303 contrasting memory success with misses, so called difference memory (DM) (Daselaar et al.,
304 2009b). The different approaches may lead to different regions being identified as ROIs, and
305 we therefore explored both approaches. In order to identify the overlap between areas that
306 deactivate during successful encoding and activate during successful retrieval, we performed
307 conjunction analyses (Nichols et al., 2005) for the source memory vs. baseline contrast, first
308 using the young adults only (18-30 years, n = 55), then the complete development sample (6-
309 30 years, n = 115), and for the complete lifespan sample (6-80 years, n = 270). We repeated
310 the analyses for the source memory vs. miss (DM) contrast using the young adults group. The
311 statistical estimates for the contrasts were false discovery rate (FDR) corrected at $P <= .05$.
312 Conjunction analyses were then performed on the resulting statistical maps, resulting in maps
313 including only the vertices that were both significantly deactivated (compared to baseline, or
314 compared to miss in the DM contrast) during encoding and activated during retrieval, i.e.
315 areas displaying an encoding retrieval flip.

316 The ROIs defined using both the baseline and DM approaches were created using the young
317 adults, and were found to be restricted to the medial PMC. These ROIs were used as masks in
318 further analyses. We extracted the average encoding and retrieval parameter estimates for all
319 conditions separately (source memory, recognition, misses, correct rejections (retrieval only),
320 false alarms (retrieval only)) for all participants. In addition to the surface-based analyses,
321 average signal during encoding and retrieval was also extracted from the left and right
322 hippocampi, automatically segmented by FreeSurfer at the individual level (Fischl et al.,
323 2002).

DTI pre-processing

The b0 images were also collected with reversed phase-encode blips, resulting in pairs of images with distortions going in opposite directions. From these pairs we estimated the susceptibility-induced off-resonance field using a method similar to what is described in (Andersson et al., 2003) as implemented in FSL (Smith et al., 2004). We then applied the estimate of the susceptibility induced off-resonance field with the eddy tool (Andersson and Sotiropoulos, 2016), which was also used to correct eddy-current induced distortions and subject head movement, and aligned all images to the first image in the series. Finally, we rotated the bvecs in accordance with the image alignments performed in the previous steps (Jenkinson et al., 2002; Leemans and Jones, 2009).

DTI analyses

In order to analyze the structural connectivity of the PMC, we used Tract Based Spatial Statistics (TBSS) available under FSL. First, the preprocessed, eddy-current, movement, and susceptibility-field corrected data were used as the input to the standard TBSS processing stream (FSL; *http://www.fmrib.ox.ac.uk/fsl).* A tensor model was first to the preprocessed diffusion data using FDT. The data was then aligned into a common space before the mean FA image was created and thinned to create a mean alignment-invariant skeleton, which represents the centers of all tracts common to the group (Rueckert et al., 1999; Smith, 2002; Smith et al., 2004; 2006; Andersson and Jenkinson, 2007; Andersson et al., 2007). We then projected the fractional anisotropy (FA) and mean diffusivity (MD) data for each individual onto this skeleton, and performed whole-brain voxel-wise analyses on the FA and MD values, and the interaction term between age and source memory. Permutation-based nonparametric cluster inference (Randomise, a part of the FSL software suite) was used, controlling for scanner, sex, age and source memory. Sex was included as a covariate of no interest in the

348 analyses, as sex differences in white matter microstructure has been reported (Inano et al.,
349 2011, Kanaan et al., 2011, Rathee et al., 2016). Five thousand permutations were performed,
350 and the results were corrected for multiple comparisons across space by threshold-free cluster
351 enhancement (Smith and Nichols, 2009; Winkler et al., 2014). The threshold level for a
352 significant difference was set at $P < .05$ (corrected). Since we also previously have observed
353 larger age-differences in PMC in this age-span for MD compared to FA (Tamnes et al., 2010),
354 and we found no significant effects of FA after statistical corrections were performed, MD
355 was chosen as the DTI measure of interest. We thus collected the average MD values from the
356 regions of the TBSS-skeleton displaying a significant age-source memory interaction, and
357 saved the residuals after regressing on scanner type and estimated movement. This corrected
358 measure was entered as the DTI measure in the multi-modal analyses.

359 The rationale for adding the microstructural measure was to investigate whether structural
360 connectivity measures added to the contributions of the PMC E/R flip in explaining age
361 differences in source memory. We used a data-driven approach for defining the DTI ROI. We
362 believe this approach, unbiased by anatomical constraints, is in line with keeping consistency
363 across analyses and modalities through the paper. While the regions that emerged as structural
364 ROIs are not directly overlapping with the PMC ROI, this does not exclude that a relationship
365 between the regions exists, and variations in e.g. WM microstructure in regions different from
366 where one finds the E/R flip could be relevant for episodic memory.

367 ***sMRI pre-processing***

368 FreeSurfer 5.3 was used for the cortical- and volumetric reconstruction of the T1-weighted
369 structural data (http://freesurfer.net). The processing steps include motion correction and
370 averaging (Reuter et al., 2010), removal of non-brain tissue (Segonne et al., 2004), automated
371 Talairach transformation and intensity correction (Sled et al., 1998). Intensity and continuity

372 information from the 3D volume are used in segmentation and deformation procedures to
373 reconstruct a gray/white and gray/cerebrospinal fluid boundary throughout the brain (Dale et
374 al., 1999; Fischl et al., 2002; 2004b). Cortical surfaces then undergo inflation, registration to a
375 spherical atlas, and identification of gyral and sulcal regions (Fischl et al., 2004a; Desikan et
376 al., 2006). Subcortical white matter and deep gray matter volumetric structures were
377 segmented, yielding volumetric measurements of the hippocampi (Fischl et al., 2002). While
378 there have been concerns that the hippocampal volume estimations from FreeSurfer differ
379 from manual segmentations (Wenger et al., 2014), associations between FreeSurfer estimated
380 volumes and manually estimated volumes are satisfactory (Schoemaker et al. 2016), and ICV-
381 adjusted age-trajectories are near identical (Schmidt et al., 2018). An experienced operator
382 manually inspected individual surfaces and segmentations for accuracy. Minor corrections
383 were needed for eight participants, mainly due to suboptimal skullstrip leading to inaccurate
384 pial surfaces, including manual edits of the brainmask for six participants, and adding
385 intensity normalization control points for two participants.

386 ***sMRI analyses***

387 Thickness maps were smoothed at FWHM 15mm prior to analyses. We assessed the
388 interaction between age and source memory on CT, with FreeSurfer's mri_glmfit, using a
389 general linear model approach, controlling for the effect of **sex** and the linear age and source
390 memory terms. We also tested for main effects of source memory on CT, controlling for sex.
391 We did include sex as a covariate in the ROI analyses, as sex is associated with differences in
392 brain structure (Raznahan et al., 2011), studies using FreeSurfer do however rarely detect sex
393 differences in mean CT or trajectories of CT development (Fjell et al., 2009, Tamnes et al.,
394 2010, Amlien et al., 2016). The analyses were performed across all vertices, and the results
395 were thresholded using pre-cached Monte Carlo simulation with a cluster-forming-threshold

396 of $p < .01$, and Bonferroni adjusted for analyses across both hemispheres. Average CT of all
397 vertices overlapping with the age-source memory interaction cluster was used as the CT
398 measure in the following analyses. We thus consider CT to be a marker for structural
399 development in this age-range. The interpretation of CT in ROI-based analyses does also
400 arguably make more neuroanatomical sense than surface area, and CT / BOLD activity
401 correlations have also been reported elsewhere (Rasser et al., 2005; Hegarty et al., 2012; Joshi
402 et al., 2016). We thus chose to use CT measures in the following analyses.

403 **Statistical analyses**

404 Polynomial regression analyses were performed to examine the continuous relationship
405 between behavior data (source memory, recognition, misses, false alarms, and d-prime) and
406 age. Similar analyses were performed on the E/R flip, and signal extracted from the PMC
407 during encoding and retrieval separately, and for left and right hippocampi, both for encoding
408 and retrieval BOLD activity and for intracranial volume (ICV) corrected residuals of
409 hippocampus volume. ICV was calculated by use of an atlas normalization procedure
410 described by Buckner et al. (2004).

411 To examine how much of the variance in source memory the combined multimodal measures
412 were able to explain, source memory, age, E/R flip, MD and CT were entered in a path
413 analysis based on structural equation modelling (SEM) (Amos, version 22). We wanted to test
414 the hypothesis that source memory performance differences are mediated through a greater
415 range of activity in the PMC region during encoding and retrieval, which in turn is dependent
416 on structural brain maturation. We also repeated the SEM modelling where we replaced the
417 E/R flip variable, and instead entered both the PMC Encoding and retrieval variables
418 separately. Direct and indirect effects were calculated. Indirect effects are calculated as the
419 product of the partial path weights from the predictor variable to the indicator variable

through other variables in the model. Indirect effects were only calculated for significant paths. Browne and Cudeck (1992) has suggested RMSEA < 0.08 to be indicative of a reasonable error of approximation, and that RMSEA < 0.05 would indicate a close fit, and models with values > 0.1 should not be employed. We thus employed the moderately conservative threshold of RMSEA < 0.05 for determining adequate model fit.

Finally, we estimated the proportion of age-related variance in source memory shared with E/R flip, MD and CT, by using the formula: $\frac{r^2_{A-C} - r^2_{A-C \cdot Bk}}{r^2_{A-C}}$, where each kth brain marker (B*k*) was partialled from the correlation between age (A) and source memory (C) (Hedden et al., 2016). In order to estimate the proportion of unique age-related variance shared with each brain marker (B), we computed partial correlation analyses using the formula: $\frac{r^2_{A-C \cdot B \in !k} - r^2_{A-C \cdot B \in k}}{r^2_{A-C}}$ where B∈*k* is the set of all brain markers (E/R flip, CT and MD), and B∈!*k* is all brain markers excluding the *k*th marker. This procedure was repeated with encoding and retrieval activity entered separately.

Results

Behavioral results

Demographics and task performance on the memory retrieval task performed during fMRI is presented in Table 2.

[Insert Table 2 around here]

Plots of behavior measures tested against age are shown in Figure 2. Source memory performance was related to age with the age trajectory forming an inverted U-shaped

function. The cubic regression was significant (R^{2adj} = .135, F[3,266] = 14.97, p < .001, $y = 0.215 + 0.0264\,x - 5.62 \times 10^{-4}\,x^2 + 3.28 \times 10^{-6}\,x^3$), and significantly better than the linear and quadratic models. Recognition was also related to age forming an inverted U-shaped function, the quadratic regression was significant (R^{2adj} = .037 F[2,267] = 6.109, p = .003, $y = 0.695 + 4.24 \times 10^{-3}\,x - 5.77 \times 10^{-6}\,x^2$), and also significantly better than the linear model. The number of recognition misses was not significantly related to age, whether a linear, quadratic or cubic model was employed (linear model, R^{2adj} < .000, F[1,268] = .938, p = .334, $y = 0.205 + 2.99 \times 10^{-4}\,x$). Number of false alarms was related to age, and the cubic regression was significant (R^{2adj} = .071, F[3,266] = 7.899, p < .001, $y = 0.0998 - 5.36 \times 10^{-3}\,x + 1.39 \times 10^{-4}\,x^2 - 9.62 \times 10^{-7}\,x^3$), with a U-shaped function, with a decrease towards the end of the age-range. The cubic model was significantly better than both the linear and quadratic models. d-prime was significantly related to age with an inverted U-shaped function, and the quadratic regression model was significant (R^{2adj} = .123, F[2,267] = 19.87, p < .001, $y = 2.47 + 0.0104\,x - 2.35 \times 10^{-4}\,x^2$), and significantly better than the linear model.

[Insert Figure 2 around here]

fMRI results

Identification of the encoding-retrieval flip

Only the vertices showing both significant (FDR-corrected) deactivation during successful source memory encoding, and activation during retrieval compared to baseline were classified as flipping voxels in the conjunction analysis. This is a stricter criterion than contrasting encoding deactivations with retrieval activations alone. We initially defined the E/R flip using

the young adult group alone. The rationale for this was that if the children, as hypothesized, showed either reduced encoding deactivations, or reduced retrieval activations, we would risk not being able to identify a region displaying the E/R flip. The conjunction analysis was performed based on group statistical maps, resulting in a map of vertices significantly deactivated during source memory encoding and significantly activated during source memory retrieval (Figure 3). The conjunction analysis left us with three regions where the E/R flip was evident, namely a cluster in the PMC bilaterally, and a posterior lateral parietal region in the left hemisphere only. The activity pattern we discovered in the posterior ventral parietal region is a region that has previously been shown to exhibit the same E/R flip pattern also found in PMC (Daselaar et al., 2009a; Gilmore et al., 2015). The PMC was defined as the region of interest a priori based on previous studies (Huijbers et al., 2012; 2013; Vannini et al., 2013; Gilmore et al., 2015), and we thus created labels of the overlap between PCM encoding deactivation and retrieval activation in the two hemispheres separately and brought these ROIs to further analyses. Individual parameter estimates were extracted from the contrast between source memory and baseline, both for encoding and retrieval. The mean signal from the left and right PMC was extracted for both sessions, and the E/R flip was defined as the resulting difference between encoding and retrieval parameter estimates, averaged across left and right PMC. Maps of significant activation or deactivation during encoding or retrieval are presented in Figure 4.

[Insert Figure3 and 4 around here]

E/R flip and source memory

E/R flip activity was related to source memory performance and the linear regression equation was significant (R^{2adj} = .016, F[1,268] = 5.407, p = .021), and the relationship between E/R flip and source memory was positive.

E/R flip and age

E/R flip activity was related to age, and the cubic regression was significant (R^{2adj} = .074, F[3,266] = 8.166, p < .001, $y = 0.0926 + 0.012\,x - 3.16 \times 10^{-4}\,x^2 + 2.18 \times 10^{-6}\,x^3$), and the model fit of the cubic regression was trending towards fitting significantly better than the quadratic and linear models (Sig F change = .059). In order to determine how the age effects of the E/R flip were driven by age-related encoding and retrieval activity patterns, we performed additional regression analyses on the subcomponents of the E/R flip measure. E/R flip ROI activity during encoding was related to age, and the cubic regression was significant (R^{2adj} = .051, F[3,266] = 5.789, p < .001, $y = 0.135 - 0.017\,x + 4.06 \times 10^{-4}\,x^2 - 2.93 \times 10^{-6}\,x^3$). The model fit of the cubic regression was significantly better than the quadratic and linear models. E/R flip ROI activity during retrieval was also related to age, but here only the linear regression was significant (R^{2adj} = .028, F[1,268] = 8.632, p = .004, $y = 0.18 - 0.00103\,x$).

[Insert Figure5 around here]

E/R flip fMRI activity was characterized by a pattern that was mirrored between development and aging (Figure 5), with increases in E/R flip until adolescence, and monotonous reductions until old age. The magnitude of the reductions through age were such that the 70-80 year olds showed E/R flip and encoding activity almost at the level of the children.

Hippocampus age trajectories

Supplementary regression analyses were performed on the BOLD signal in bilateral hippocampus and age (Figure 6). Activity in the right Hippocampus during recall was positively related to retrieval success and the cubic regression was significant (R^{2adj} = .031, F[3,266] = 3.86, p = .010, $y = 0.803 + 0.8\,x - 2.761\,x^2 + 2.071\,x^3$). Hippocampus

activity during both encoding and retrieval was significantly related to age. For encoding, the cubic regression was significant for right hippocampus (R^{2adj} = .031, F[3,266] = 3.874, p = .009, $y = 0.104 - 0.00511\,x + 0.000115\,x^2 - 8.05 \times 10^{-7}\,x^3$), and for retrieval, left (R^{2adj} = .012, F[3,266] = 13.43, p < .001, $y = 0.204 - 0.0155\,x + 0.000394\,x^2 - 2.92 \times 10^{-6}\,x^3$), and right Hippocampus (R^{2adj} = .010, F[3,266] = 11.5, p < .001, $y = 0.175 - 0.0133\,x + 0.000334\,x^2 - 2.45 \times 10^{-6}\,x^3$). The model fit of the cubic regressions were significantly better than the quadratic and linear models. The shape of the regression function showed a slight initial decrease with little change through middle age, before another dip in old age.

Hippocampus volume (ICV residuals) followed an inverted U-trajectory through the lifespan (Figure 7), and the quadratic regression was significant (Left: $\mathbf{R^{2adj}}$ = .27, F[2,252] = 47.74, p < .001, $y = -0.322 + 0.0543\,x - 0.000893\,x^2$; Right: $\mathbf{R^{2adj}}$ = .24, F[2,252] = 40.2, p < .001, $y = -0.101 + 0.0406\,x - 0.000729\,x^2$). ICV corrected Hippocampus volumes (residuals) were significantly related to source memory (Left: $\mathbf{R^2}$ = .042, p < .001; Right: $\mathbf{R^2}$ = .027, p = .009), but when corrected for the linear and quadratic age terms, the relationship was not significant (Left: p = .655; Right: p = .998). Both the fMRI and volumetric results are consistent with earlier reports on lifespan changes in hippocampus volume and activity (Van Petten, 2004; Østby et al., 2009; Walhovd et al., 2011; Wierenga et al., 2014a).

[Insert Figure 6 and 7 around here]

Alternative E/R flip ROI

We tested different approaches for defining the E/R flip ROI. First, we generated the E/R flip ROIs using a DM approach (contrasting source memory with misses). The resulting ROIs are

shown in Figure 8 (top left). In line with previous literature, we found that the ROIs extended spatially over a larger area than the implicit baseline approach (Figure 8, middle left). The spatially more restricted E/R flip ROI defined using the baseline contrast was almost completely overlapped by the DM ROI. Comparing lifespan trajectories of the E/R flip based on the two different strategies (Figure 8, top right) we found that they yielded similar overall patterns, but with a longer apparent increase in E/R flip magnitude with the larger DM based ROI. Baseline vs. DM approaches are discussed in-depth in a review paper by Gilmore et al. (2015), who defines the E/R flip as "a regional BOLD response pattern in which the direction of evoked activity, relative to resting baseline, flips between encoding and retrieval." Following Gilmore et al. (2015), the baseline defined ROI was used for all other analyses.

Further, as alternatives to define the E/R flip ROI based on the young adults only, we ran additional analyses defining the E/R flip ROI using both the full development sample (6-30 years, n = 105), and the complete lifespan sample (6-80 years, n = 270). The resulting ROIs can be seen in Figure 8, bottom row. The main findings were progressively larger ROIs as we increased sample size and age range in both directions. While this pattern can be influenced by different activity patterns in development and aging, differences in statistical power between analyses may also affect the size of the ROIs.

Given that the ROI based on the young adults included almost only vertices common to the ROIs defined based on the alternative samples, and our hypothesis that the ability to modulate activity in the PMC is not yet fully developed in children and may be reduced in aging, further analyses were based on the ROI defined in the young adults sample (18-30 years).

[Insert Figure 8 around here]

Multi-modal Development Model

In order to quantify the influence of E/R flip and brain structure on memory development, we constructed a model containing structural measures relevant to memory development, in addition to age, source memory, and E/R flip. We extracted CT and MD measures from the brain regions showing significant interaction with age, i.e. the regions where the relationship between the brain measures and source memory were not constant across age.

Cortical Thickness

CT was extracted from a posterior cluster which remained significant after correcting for multiple comparisons, encompassing cuneus and calcarine sulcus (Figure 9, top). The interaction was positive, meaning the source memory - CT relationship increased with age. Thickness in this ROI correlated negatively with age ($r = -.45$, $p < .001$), source memory ($r = -.26$, $p = .013$), and E/R flip ($r = -.22$, $p = .038$) in the developmental subsample (Table 3). As background information, we also tested the effect of source memory on CT, vertex-wise across the cortical surfaces. A main effect of source memory on CT was found in two left hemisphere clusters when controlling for the effect of **sex**, one cluster encompassing lingual gyrus, and one cluster on the border of precuneus, isthmus cingulate, and posterior cingulate cortex (Figure 9, bottom).

Mean Diffusivity

MD was extracted from a region in the left medial temporal lobe, left longitudinal fasciculus, and corticospinal tract, where the age-source memory interaction analysis revealed increased source memory - MD relation with age (Figure 10). MD did not correlate significantly with any other variable of interest in the developmental subsample (Table 3), and there were no main effects of source memory on MD that remained significant after correcting for multiple comparisons.

[Insert Figure 9 and 10 around here]

In order to estimate the proportion of age variance in source memory that could be accounted for by the individual brain measures, a series of partial correlations were conducted (Table 4). E/R flip, MD and CT together accounted for 55.0 % of the age-related variance in source memory performance. Of this, 8.1 % of the age-related variance in source memory was uniquely accounted for by the E/R flip, 0.4 % by MD and 28.9 % by CT, while the rest was accounted for by more than one of the measures together. E/R flip shared 24.5 % of its age-related variance with the other measures, MD 6.0 %, and CT 44.7 %. An identical analysis, with the PMC Encoding and retrieval variables entered separately as in SEM C, resulted in an overall reduction in the age-related variance in source memory (26.6%) we were able to account for. Part of the reduction could likely be explained by variance suppression effects on the age-source memory relationship by encoding/retrieval activation, indicated by negative shared variance (Encoding: -15.2%, Retrieval: -11.3%).

Aiming to separate the age-related variance in source memory that could be explained by each of the functional and structural measures (Figure 11), we performed path analyses (Figure 12). Age was entered as the only exogenous variable, source memory was the endogenous variable, and E/R flip, MD, and CT were entered as mediating variables. Directional paths were drawn from age to all other variables, to source memory from all other variables, and to E/R flip from all other variables except source memory. We revised the initial model (Figure 12A) in iterations, trimming the arrow with lowest critical ratio until only significant relationships ($p < .05$) remained. In the final model (Figure 12B), source memory was related to age ($\beta = 0.28$, 95% CI: .068 ~ .494) and E/R flip ($\beta = 0.24$, 95% CI: .030 ~ .459). CT was also related to age ($\beta = -0.45$, 95% CI: -.604 ~ -.252) and E/R flip ($\beta = -0.22$, 95% CI: -.412 ~ -.012). Age exerted a small indirect effect on source memory through CT and E/R flip ($\beta =$

0.024, 95% CI: .002 ~ .086).The final model yielded a satisfactory fit to the data with a root mean square error of approximation (RMSEA) value of .048 (PCLOSE = .376, relative chi-square = 1.21, CFI = .989, NFI = .943).

We finally created a SEM where we instead of the E/R flip variable entered both PMC Encoding and retrieval variables separately, with arrows from age to all variables, from MD and CT to all other variables but age, and from PMC encoding and retrieval to source memory, with an additional arrow from PMC encoding to PMC retrieval. Using identical procedures for model trimming as for the E/R flip analyses, the final model (Figure 12C) showed that retrieval activity is most directly related to source memory, and encoding activity was indirectly related to source memory through its relationship with retrieval. Age was directly related to source memory (β = 0.32, 95% CI: .107 ~ .505), encoding (β = -0.22, 95% CI: -.414 ~ -.007), and CT (β = -0.45, 95% CI: -.604 ~ -.252), and there were small indirect effects of age on source memory through the encoding / retrieval path (β = -0.03), and through the CT-retrieval path (β = -0.03). Encoding was directly related to retrieval (β = .41, 95% CI: .217 ~ .557), and indirectly to source memory through retrieval (β = .15, 95% CI: .060 ~ .259). CT was directly related to retrieval (β = -0.20, 95% CI: -.372 ~ -.010), and indirectly to source memory through retrieval (β = -0.075, 95% CI: -.174 ~ -.011). The final iteration of this model did also provide a good fit to the data with a root mean square error of approximation (RMSEA) value of 0 (PCLOSE = .969, relative chi-square = .266, CFI = 1, NFI = .99).

[Insert Figure 11 and 12 around here]

Discussion

The ability to recall episodic memories is dependent on the dynamic range of neural activity in the PMC, and the interplay between neural processes occurring during encoding and retrieval (Daselaar et al., 2009a; Vannini et al., 2010; W Huijbers, 2012; Huijbers et al., 2013). Here we demonstrate that efficient functional modulation of the PMC is not yet fully developed in pre-adolescent children. The combination of age, E/R flip, CT and MD explained 17 % of the variance in source memory performance, but more than 50 % of the age-related performance differences. These age-related differences indicate that the functional development of the PMC and related brain regions is important for the emergence of the ability to encode and recollect episodic memories.

Young adults and adolescents deactivated the PMC during successful source memory encoding, but this deactivation was absent in children. The lack of deactivations in children is consistent with Chai et al. (2014), who reported less encoding-related deactivation in posterior parietal DMN in children compared to older participants. The deactivations already seen in adolescents indicate that emergence of the ability to modulate PMC activity during memory operations is likely a central feature of brain development ongoing at this age.

Activity in the PMC shares many similarities with the rest of the DMN, and deactivations may reflect attention orientated outward, i.e. attending to external stimuli in the encoding task (Huijbers et al., 2012). Deactivation of the DMN during encoding, possibly in order to allocate cognitive resources to task-oriented processes, is associated with better subsequent memory performance (Kim, 2011). Activation of the DMN occurs when attention is oriented inwards towards one's own mental processes, and is associated with successful retrieval of episodic memories (Kim et al., 2010). Likely, the ability of the PMC to dynamically toggle

645 between deactivation and activation is important to the development of source memory, in
646 addition to activation/deactivation strength alone. An intriguing question is if the neural
647 processes occurring in the PMC during encoding and retrieval reflect fundamentally different
648 tasks served by the same cortical area, seen as bi-polar activation patterns, or rather reflect
649 varying intensity of a unitary task or process.

650 ***E/R flip through the life-span***

651 Reductions in E/R flip have been demonstrated in aging (Vannini et al., 2013), and we add to
652 this by showing the E/R flip trajectory through the lifespan. E/R flip trajectory steeply rose
653 with age until early adulthood, before it declined monotonously through the rest of life. The
654 encoding deactivations in the PMC seemed to follow a similar pattern, but peaking later. The
655 70-80 year old participants displayed similar levels of encoding deactivations as children.
656 While tempting to assume that age-related differences in development (apparent increase) and
657 aging (apparent decrease) reflect similar mechanisms, we do not know what causes the
658 differences in BOLD responses with age. We need targeted studies focusing on the exact
659 cognitive and neural mechanisms underlying PMC activity modulation, as well as better
660 knowledge about possible age-effects on neurovascular coupling. For instance, changes in
661 factors such as cerebral blood flow, volume and oxygen consumption may influence this
662 relationship. Different mechanisms may also be active through different phases of life
663 (D'Esposito et al., 2003). Nevertheless, the E/R flip was related to source memory
664 performance across the sample, also when controlling for age, indicating that modulation of
665 activity in this region is relevant for the ability to form and retrieve episodic memories.

666 ***PMC as a network hub***

667 The age-related functional differences in the PMC might be related to its communication with
668 other regions and networks, not only local properties of the region. The PMC shows

connectivity with DMN nodes (Cauda et al., 2010), but also to other intrinsically connected networks, including task-positive fronto-parietal networks which show the opposite activity patterns to the DMN (Fox et al., 2005). The PMC has wide structural connections (Hagmann et al., 2008), and the resting state connectivity has been shown to correspond with structural connectivity measured by DTI (Greicius et al., 2009; Gordon et al., 2011; Horn et al., 2014). Assuming that PMC flexibility during encoding and retrieval is related to network interactions with other DMN nodes, we hypothesized that WM microstructure would relate to E/R flip and source memory performance. While we found a significant interaction between source memory and age on the structural connectivity measures (MD) in left SLF and left temporal lobe region, MD in this region was related to retrieval activity and E/R flip on a trend level only ($p \sim .10$) and not to source memory.

A multi-modal imaging model of episodic memory development

CT contributed indirectly to source memory performance through the E/R flip, and CT was heavily influenced by age. Consistent with prior reports that consistently show maturation of CT as thinning of the cortex (Brown and Jernigan, 2012; Mutlu et al., 2013; Nguyen et al., 2013; Burgaleta et al., 2014; Zielinski et al., 2014; Wierenga et al., 2014b) we evinced reduction in cortical thickness with advanced age. Hence, in addition to age, both cortical thickness in a sensory region associated with the memory task, and modulation of activity in the PMC, accounted for parts of the variance in source memory attributed to age. The source memory – thickness correlation in early visual cortices was significantly larger in young participants than in older participants. Retrieval of episodic components depends on re-activation of respective sensory regions that were active during encoding (Nyberg et al., 2000). The memory task presumably involved mental imagery, and the interaction of age and

source memory performance may reflect maturation of cortical regions needed for successful encoding and retrieval of visual episodic memories.

E/R flip, MD and CT shared some age-related variance in source memory, but only E/R flip and CT explained unique parts of the variance, 8.1 % and 28.9 % respectively. Decomposing the E/R flip into encoding and retrieval activity showed that modulation of activity between encoding and retrieval may provide a unique contribution to explain the age-source memory development, more so than the separate measures alone. In similar analyses in an aging sample, Hedden et al. (2016) also reported absence of unique contributions from DTI to age-related variance in episodic memory. Instead of using apriori defined global brain measures employed by Hedden and colleagues, we used measures tailored to the study, i.e. extracted from regions where the relationship with source memory changed with age. While we expected this to increase specificity to source memory for MD, we did not detect a significant relationship. The DTI data for the youngest children were however collected in advance of the fMRI data, which may contribute as a limitation to the null findings. Nonetheless, when combined in the present study, neuroimaging measures explain a major part of episodic memory development in this age-range.

Limitations and future directions

Although the sample size is 270, only 21 children were aged 14 years or younger, which limits the precision in estimating age-trajectories of the youngest part of the sample. Also, head motion is related to age and can potentially influence the results (Figure 1), even if precautions are taken at several stages in the analyses. The study design is cross-sectional, and the results represent age-differences. Interpretation of brain-behavior relationships in periods of brain development may pose challenges, not least when structure and connectivity is considered in addition to brain activity alone (McCormick et al., 2017). The participants in

716 the study were healthy and cognitively fit. Selection bias (for example withdrawal- and
717 survivor bias) and the cross-sectional design may have led to underestimation of the decline
718 with age, particularly in older parts of the sample (see Nyberg et al. (2010)). A longitudinal
719 replication attempt would be highly useful to estimate the size of cohort-effects and other
720 limitations of the study design.

721 The method for defining E/R flip resulted in small ROIs, located on the edge of DMN nodes,
722 and the parietal memory network. These are neuroanatomically and functionally distinct
723 regions, and both anatomical variations and differences in parameters used for defining the
724 ROIs, may affect the overlap between ROIs and networks with possibly opposing activity
725 patterns. Worth noting is that the E/R flip possibly occurs on border regions between
726 functionally distinct networks, and the behavior reflected as E/R flip may represent
727 interaction or integration of activity in anatomically adjacent networks.

728 Future studies should aim to decompose the E/R flip further, to gain better understanding of
729 the E/R flip function in relation to functional and structural brain networks.

730 ***Conclusion***

731 The present results show that pre-adolescence children show less modulation of neural
732 activity in the PMC during encoding and retrieval operations. The E/R flip does not reach its
733 peak until adolescence, and decreases from adulthood through old age. Increase in the
734 dynamic modulation of PMC activity appeared to continue into adulthood, and then declined
735 monotonously. Ultimately, between 70 and 80 years, a child-like pattern of PMC modulation
736 was observed. A multi-modal model could account for more than half of the age-related
737 improvements in episodic memory performance in children and adolescents. The findings
738 suggest a role of PMC in both emergence and decline of episodic memory.

739

References

Amlien IK, Fjell AM, Tamnes CK, Grydeland H, Krogsrud SK, Chaplin TA, Rosa MGP, Walhovd KB (2016) Organizing Principles of Human Cortical Development-Thickness and Area from 4 to 30 Years: Insights from Comparative Primate Neuroanatomy. Cereb Cortex 26:257–267.

Andersson JLR, Jenkinson M (2007) Non-linear optimisation. FMRIB technical report TR07JA1. Available at: http://fsl.fmrib.ox.ac.uk/analysis/techrep/tr07ja1/tr07ja1.pdf [Accessed December 12, 2016].

Andersson JLR, Jenkinson M, Smith S (2007) Non-linear registration, aka Spatial normalisation FMRIB technical report TR07JA2. Available at: https://www.fmrib.ox.ac.uk/analysis/techrep/tr07ja2/tr07ja2.pdf [Accessed December 12, 2016].

Andersson JLR, Skare S, Ashburner J (2003) How to correct susceptibility distortions in spin-echo echo-planar images: application to diffusion tensor imaging. Neuroimage 20:870–888.

Andersson JLR, Sotiropoulos SN (2016) An integrated approach to correction for off-resonance effects and subject movement in diffusion MR imaging. Neuroimage 125:1063–1078.

Beckmann CF, Smith SM (2004) Probabilistic independent component analysis for functional magnetic resonance imaging. IEEE Trans Med Imaging 23:137–152.

Blüml S, Wisnowski JL, Nelson MD, Paquette L, Gilles FH, Kinney HC, Panigrahy A (2013) Metabolic maturation of the human brain from birth through adolescence: insights from in vivo magnetic resonance spectroscopy. Cereb Cortex 23:2944–2955.

Brown TT, Jernigan TL (2012) Brain development during the preschool years. Neuropsychol Rev 22:313–333.

Browne MW, Cudeck R (1992) Alternative Ways of Assessing Model Fit. Sociological Methods & Research 21:230–258.

Buckner RL, Andrews Hanna JR, Schacter DL (2008) The brain's default network. Annals of the New York Academy of Sciences 1124:1–38.

Buckner RL, Head D, Parker J, Fotenos AF, Marcus D, Morris JC, Snyder AZ (2004) A unified approach for morphometric and functional data analysis in young, old, and demented adults using automated atlas-based head size normalization: reliability and validation against manual measurement of total intracranial volume. Neuroimage 23:724–738.

Burgaleta M, Johnson W, Waber DP, Colom R (2014) Cognitive ability changes and dynamics of cortical thickness development in healthy children and adolescents. Neuroimage 84:810–819.

Cauda F, Geminiani G, D'Agata F, Sacco K, Duca S, Bagshaw AP, Cavanna AE (2010) Functional Connectivity of the Posteromedial Cortex. PLoS ONE 5:–11.

Chai XJ, Ofen N, Gabrieli JDE, Whitfield-Gabrieli S (2014) Development of deactivation of the default-mode network during episodic memory formation. Neuroimage 84:932–938.

D'Esposito M, Deouell LY, Gazzaley A (2003) Alterations in the bold FMRI signal with ageing and disease: A challenge for neuroimaging. Nat Rev Neurosci 4:863–872.

Dale AM, Fischl B, Sereno MI (1999) Cortical surface-based analysis. I. Segmentation and surface reconstruction. Neuroimage 9:179–194.

Daselaar SM, Prince SE, Cabeza R (2004) When less means more: deactivations during encoding that predict subsequent memory. Neuroimage 23:921–927.

Daselaar SM, Prince SE, Dennis NA, Hayes SM, Kim H, Cabeza R (2009a) Posterior Midline and Ventral Parietal Activity is Associated with Retrieval Success and Encoding Failure. Front Hum Neurosci 3:13.

Daselaar SM, Prince SE, Dennis NA, Hayes SM, Kim H, Cabeza R (2009b) Posterior midline and ventral parietal activity is associated with retrieval success and encoding failure. Front Hum Neurosci 3.

Degnan AJ, Ceschin R, Lee V, Schmithorst VJ, Blüml S, Panigrahy A (2014) Early metabolic development of posteromedial cortex and thalamus in humans analyzed via in vivo quantitative magnetic resonance spectroscopy. J Comp Neurol 522:3717–3732.

Desikan RS, Ségonne F, Fischl B, Quinn BT, Dickerson BC, Blacker D, Buckner RL, Dale AM, Maguire RP, Hyman BT, Albert MS, Killiany RJ (2006) An automated labeling system for subdividing the human cerebral cortex on MRI scans into gyral based regions of interest. Neuroimage 31:968–980.

Duarte A, Graham KS, Henson RN (2010) Age-related changes in neural activity associated with familiarity, recollection and false recognition. Neurobiol Aging 31:1814–1830.

Fischl B, Salat DH, Busa E, Albert M, Dieterich M, Haselgrove C, van der Kouwe A, Killiany R, Kennedy D, Klaveness S, Montillo A, Makris N, Rosen B, Dale AM (2002) Whole brain segmentation: automated labeling of neuroanatomical structures in the human brain. Neuron 33:341–355.

Fischl B, Salat DH, van der Kouwe AJW, Makris N, Ségonne F, Quinn BT, Dale AM (2004a) Sequence-independent segmentation of magnetic resonance images. Neuroimage 23:S69–S84.

Fischl B, van der Kouwe A, Destrieux C, Halgren E, Ségonne F, Salat DH, Busa E, Seidman LJ, Goldstein J, Kennedy D, Caviness V, Makris N, Rosen B, Dale AM (2004b) Automatically parcellating the human cerebral cortex. Cereb Cortex 14:11–22.

Fox MD, Snyder AZ, Vincent JL, Corbetta M, Van Essen DC, Raichle ME (2005) The human brain is intrinsically organized into dynamic, anticorrelated functional networks. Proc Natl Acad Sci USA 102:9673–9678.

Gao W (2009) Evidence on the emergence of the brain's default network from 2-week-old to 2-year-old healthy pediatric subjects. Proceedings of the National Academy of Sciences of the United States of America 106:6790–6795.

Ghetti S, Bunge SA (2012) Neural changes underlying the development of episodic memory during middle childhood. Developmental cognitive neuroscience 2:381–395.

Gilmore AW, Nelson SM, McDermott KB (2015) A parietal memory network revealed by multiple MRI methods. Trends Cogn Sci (Regul Ed) 19:534–543.

Gordon EM, Lee PS, Maisog JM, Foss Feig J, Billington ME, VanMeter J, Vaidya CJ (2011) Strength of default mode resting-state connectivity relates to white matter integrity in children. Developmental Science 14:738–751.

Greicius MD, Supekar K, Menon V, Dougherty RF (2009) Resting-state functional connectivity reflects structural connectivity in the default mode network. Cereb Cortex 19:72–78.

Griffanti L, Salimi-Khorshidi G, Beckmann CF, Auerbach EJ, Douaud G, Sexton CE, Zsoldos E, Ebmeier KP, Filippini N, Mackay CE, Moeller S, Xu J, Yacoub E, Baselli G, Ugurbil K, Miller KL, Smith SM (2014) ICA-based artefact removal and accelerated fMRI acquisition for improved resting state network imaging. Neuroimage 95:232–247.

Hagmann P, Cammoun L, Gigandet X, Meuli R, Honey CJ, Van J Wedeen, Sporns O (2008) Mapping the Structural Core of Human Cerebral Cortex Friston KJ, ed. PLOS Biol 6:e159.

Hedden T, Schultz AP, Rieckmann A, Mormino EC, Johnson KA, Sperling RA, Buckner RL (2016) Multiple Brain Markers are Linked to Age-Related Variation in Cognition. Cereb Cortex 26:1388–1400.

Hegarty CE, Foland-Ross LC, Narr KL, Townsend JD, Bookheimer SY, Thompson PM, Altshuler LL (2012) Anterior cingulate activation relates to local cortical thickness. Neuroreport:1.

Horn A, Ostwald D, Reisert M, Blankenburg F (2014) The structural-functional connectome and the default mode network of the human brain. Neuroimage 102 Pt 1:142–151.

Huijbers W, Schultz AP, Vannini P, McLaren DG, Wigman SE, Ward AM, Hedden T, Sperling RA (2013) The Encoding/Retrieval Flip: Interactions between Memory Performance and Memory Stage and Relationship to Intrinsic Cortical Networks. J Cogn Neurosci 25:1163–1179.

Huijbers W, Vannini P, Sperling RA, C M P, Cabeza R, Daselaar SM (2012) Explaining the encoding/retrieval flip: memory-related deactivations and activations in the posteromedial cortex. Neuropsychologia 50:3764–3774.

Inano S, Takao H, Hayashi N, Abe O, Ohtomo K (2011) Effects of age and gender on white matter integrity. Am J Neuroradiol 32:2103–2109.

Jenkinson M, Bannister P, Brady M, Smith S (2002) Improved optimization for the robust and

accurate linear registration and motion correction of brain images. Neuroimage 17:825–841.

Joshi SH, Vizueta N, Foland-Ross L, Townsend JD, Bookheimer SY, Thompson PM, Narr KL, Altshuler LL (2016) Relationships Between Altered Functional Magnetic Resonance Imaging Activation and Cortical Thickness in Patients With Euthymic Bipolar I Disorder. Biological Psychiatry: Cognitive Neuroscience and Neuroimaging 1:507–517.

Kanaan RA, Allin M, Picchioni M, Barker GJ, Daly E, Shergill SS, Woolley J, McGuire PK (2012) Gender Differences in White Matter Microstructure Gong Q, ed. PLoS ONE 7:e38272.

Kim H (2011) Neural activity that predicts subsequent memory and forgetting: A meta-analysis of 74 fMRI studies. Neuroimage 54:2446–2461.

Kim H (2013) Differential neural activity in the recognition of old versus new events: an activation likelihood estimation meta-analysis. Hum Brain Mapp 34:814–836.

Kim H, Daselaar SM, Cabeza R (2010) Overlapping brain activity between episodic memory encoding and retrieval: roles of the task-positive and task-negative networks. Neuroimage 49:1045–1054.

Leemans A, Jones DK (2009) The B-matrix must be rotated when correcting for subject motion in DTI data. Magn Reson Med 61:1336–1349.

Lundstrom BN, Petersson KM, Andersson J, Johansson M, Fransson P, Ingvar M (2003) Isolating the retrieval of imagined pictures during episodic memory: activation of the left precuneus and left prefrontal cortex. Neuroimage 20:1934–1943.

McCormick EM, Qu Y, Telzer EH (2017) Activation in Context: Differential Conclusions Drawn from Cross-Sectional and Longitudinal Analyses of Adolescents' Cognitive Control-Related Neural Activity. Front Hum Neurosci 11:61.

Mutlu AK, Schneider M, Debbané M, Badoud D, Eliez S, Schaer M (2013) Sex differences in thickness, and folding developments throughout the cortex. Neuroimage 82:200–207.

Nguyen T-V, McCracken J, Ducharme S, Botteron KN, Mahabir M, Johnson W, Israel M, Evans AC, Karama S, Brain Development Cooperative Group (2013) Testosterone-related cortical maturation across childhood and adolescence. Cereb Cortex 23:1424–1432.

Nichols T, Brett M, Andersson J, Wager T, Poline J-B (2005) Valid conjunction inference with the minimum statistic. Neuroimage 25:653–660.

Nyberg L, Habib R, McIntosh AR, Tulving E (2000) Reactivation of encoding-related brain activity during memory retrieval. Proc Natl Acad Sci USA 97:11120–11124.

Nyberg L, Salami A, Andersson M, Eriksson J, Kalpouzos G, Kauppi K, Lind J, Pudas S, Persson J, Nilsson L-G (2010) Longitudinal evidence for diminished frontal cortex function in aging. Proc Natl Acad Sci USA 107:22682–22686.

Ofen N, Kao Y-C, Sokol-Hessner P, Kim H, Whitfield-Gabrieli S, Gabrieli JDE (2007) Development of the declarative memory system in the human brain. Nat Neurosci 10:1198–1205.

Ollinger JM, Shulman GL, Corbetta M (2001) Separating processes within a trial in event-related functional MRI. Neuroimage 13:210–217.

Otten LJ, Rugg MD (2001) Task-dependency of the neural correlates of episodic encoding as measured by fMRI. Cereb Cortex 11:1150–1160.

Power JD, Fair DA, Schlaggar BL, Petersen SE (2010) The Development of Human Functional Brain Networks. Neuron 67:735–748.

Raichle ME, MacLeod AM, Snyder AZ, Powers WJ, Gusnard DA, Shulman GL (2001) A default mode of brain function. Proc Natl Acad Sci USA 98:676–682.

Rasser PE, Johnston P, Lagopoulos J, Ward PB, Schall U, Thienel R, Bender S, Toga AW, Thompson PM (2005) Functional MRI BOLD response to Tower of London performance of first-episode schizophrenia patients using cortical pattern matching. Neuroimage 26:941–951.

Rathee R, Rallabandi VPS, Roy PK (2016) Age-related Differences in White Matter Integrity in Healthy Human Brain: Evidence from Structural Mri and Diffusion Tensor Imaging. Magnetic Resonance Insights 9:MRI.S39666.

Reuter M, Rosas HD, Fischl B (2010) Highly accurate inverse consistent registration: a robust approach. Neuroimage 53:1181–1196.

Rueckert D, Sonoda LI, Hayes C, Hill DLG, Leach MO, Hawkes DJ (1999) Nonrigid registration using free-form deformations: application to breast MR images. IEEE Trans Med Imaging 18:712–721.

Salimi-Khorshidi G, Douaud G, Beckmann CF, Glasser MF, Griffanti L, Smith SM (2014) Automatic denoising of functional MRI data: Combining independent component analysis and hierarchical fusion of classifiers. Neuroimage 90:449–468.

Schmidt MF, Storrs JM, Freeman KB, Jack CR, Turner ST, Griswold ME, Mosley TH (2018) A comparison of manual tracing and FreeSurfer for estimating hippocampal volume over the adult lifespan. Hum Brain Mapp 39:2500–2513.

Schoemaker D, Buss C, Head K, Sandman CA, Davis EP, Chakravarty MM, Gauthier S, Pruessner JC (2016) Hippocampus and amygdala volumes from magnetic resonance images in children: Assessing accuracy of FreeSurfer and FSL against manual segmentation. Neuroimage 129:1–14.

Segonne F, Dale AM, Busa E, Glessner M, Salat D, Hahn HK, Fischl B (2004) A hybrid approach to the skull stripping problem in MRI. Neuroimage 22:1060–1075.

Serences JT (2004) A comparison of methods for characterizing the event-related BOLD timeseries in rapid fMRI. Neuroimage 21:1690–1700.

927 Sled JG, Zijdenbos AP, Evans AC (1998) A nonparametric method for automatic correction
928 of intensity nonuniformity in MRI data. IEEE Trans Med Imaging 17:87–97.

929 Smith SM (2002) Fast robust automated brain extraction. Hum Brain Mapp 17:143–155.

930 Smith SM, Jenkinson M, Johansen-Berg H, Rueckert D, Nichols TE, Mackay CE, Watkins
931 KE, Ciccarelli O, Cader MZ, Matthews PM, Behrens TEJ (2006) Tract-based spatial
932 statistics: voxelwise analysis of multi-subject diffusion data. Neuroimage 31:1487–1505.

933 Smith SM, Jenkinson M, Woolrich MW, Beckmann CF, Behrens TEJ, Johansen-Berg H,
934 Bannister PR, De Luca M, Drobnjak I, Flitney DE, Niazy RK, Saunders J, Vickers J,
935 Zhang Y, De Stefano N, Brady JM, Matthews PM (2004) Advances in functional and
936 structural MR image analysis and implementation as FSL. Neuroimage 23 Suppl 1:S208–
937 S219.

938 Sneve MH, Grydeland H, Nyberg L, Bowles B, Amlien IK, Langnes E, Walhovd KB, Fjell
939 AM (2015) Mechanisms Underlying Encoding of Short-Lived Versus Durable Episodic
940 Memories. J Neurosci 35:5202–5212.

941 Supekar K, Musen M, Menon V (2009) Development of Large-Scale Functional Brain
942 Networks in Children. Plos Biology 7.

943 Tamnes CK, Walhovd KB, Dale AM, Østby Y, Grydeland H, Richardson G, Westlye LT,
944 Roddey JC, Hagler DJ Jr., Due-Tønnessen P, Holland D, Fjell AM (2013) Brain
945 development and aging: Overlapping and unique patterns of change. Neuroimage 68:63–
946 74.

947 Tamnes CK, Østby Y, Fjell AM, Westlye LT, Due-Tønnessen P, Walhovd KB (2010) Brain
948 maturation in adolescence and young adulthood: regional age-related changes in cortical
949 thickness and white matter volume and microstructure. Cereb Cortex 20:534–548.

950 Thirion B, Pinel P, Meriaux S, Roche A, Dehaene S, Poline J-B (2007) Analysis of a large
951 fMRI cohort: Statistical and methodological issues for group analyses. Neuroimage
952 35:105–120.

953 Van Petten C (2004) Relationship between hippocampal volume and memory ability in
954 healthy individuals across the lifespan: review and meta-analysis. Neuropsychologia
955 42:1394–1413.

956 Vannini P, Hedden T, Huijbers W, Ward A, Johnson KA, Sperling RA (2013) The Ups and
957 Downs of the Posteromedial Cortex: Age- and Amyloid-Related Functional Alterations of
958 the Encoding/Retrieval Flip in Cognitively Normal Older Adults. Cereb Cortex 23:1317–
959 1328.

960 Vannini P, O'Brien J, O'Keefe K, Pihlajamaki M, LaViolette P, Sperling RA (2010) What
961 Goes Down Must Come Up: Role of the Posteromedial Cortices in Encoding and
962 Retrieval. Cereb Cortex 21:22–34.

963 Vidal-Piñeiro D, Sneve MH, Storsve AB, Roe JM, Walhovd KB, Fjell AM (2017) Neural
964 correlates of durable memories across the adult lifespan: brain activity at encoding and
965 retrieval. Neurobiol Aging 0:20–33.

Wagner AD, Davachi L (2001) Cognitive neuroscience: Forgetting of things past. Current Biology 11:R964–R967.

Wagner AD, Shannon BJ, Kahn I, Buckner RL (2005) Parietal lobe contributions to episodic memory retrieval. Trends Cogn Sci (Regul Ed) 9:445–453.

Walhovd KB, Westlye LT, Amlien I, Espeseth T, Reinvang I, Raz N, Agartz I, Salat DH, Greve DN, Fischl B, Dale AM, Fjell AM (2011) Consistent neuroanatomical age-related volume differences across multiple samples. Neurobiol Aging 32:916–932.

Wenger E, Mårtensson J, Noack H, Bodammer NC, Kühn S, Schaefer S, Heinze HJ, Düzel E, Bäckman L, Lindenberger U, Lövdén M (2014) Comparing manual and automatic segmentation of hippocampal volumes: reliability and validity issues in younger and older brains. Hum Brain Mapp 35:4236–4248.

Wierenga L, Langen M, Ambrosino S, van Dijk S, Oranje B, Durston S (2014a) Typical development of basal ganglia, hippocampus, amygdala and cerebellum from age 7 to 24. Neuroimage 96:67–72.

Wierenga LM, Langen M, Oranje B, Durston S (2014b) Unique developmental trajectories of cortical thickness and surface area. Neuroimage 87:120–126.

Wonderlick JS, Ziegler DA, Hosseini-Varnamkhasti P, Locascio JJ, Bakkour A, van der Kouwe A, Triantafyllou C, Corkin S, Dickerson BC (2009) Reliability of MRI-derived cortical and subcortical morphometric measures: effects of pulse sequence, voxel geometry, and parallel imaging. Neuroimage 44:1324–1333.

Zielinski BA, Prigge MBD, Nielsen JA, Froehlich AL, Abildskov TJ, Anderson JS, Fletcher PT, Zygmunt KM, Travers BG, Lange N, Alexander AL, Bigler ED, Lainhart JE (2014) Longitudinal changes in cortical thickness in autism and typical development. Brain 137:1799–1812.

Østby Y, Tamnes CK, Fjell AM, Westlye LT, Due-Tønnessen P, Walhovd KB (2009) Heterogeneity in subcortical brain development: A structural magnetic resonance imaging study of brain maturation from 8 to 30 years. J Neurosci 29:11772–11782.

Figure legends

Figure 1. Estimated relative motion across all runs, for all included participants. Fit line using R's loess function with 1.3 span, and standard error marked as shaded area.

Figure 2. Scatterplots showing the relationships between age and (left to right): Source memory, recognition memory, recognition misses, false alarms, and d-prime score, from 6 to 80 years. Fit line using R's loess function with 1.3 span, and standard error marked as shaded area.

Figure 3. Conjunction analysis results based on 55 young adult participants (18.6-30.4 years). Top row: Areas shown in blue are significantly deactivated during successful source memory encoding. Bottom row: Areas shown in red are significantly activated during successful source memory retrieval. Middle row: Green areas represent the area of overlap: The Encoding/Retrieval Flip. Significant areas are FDR corrected at $p < .05$.

Figure 4. Areas showing significant source memory success activation contrasted with baseline shown in warm colors, deactivations in cool colors, during encoding (top), and retrieval (bottom). Only vertices significant after FDR correction at the $p < .05$ level are shown.

Figure 5. From left to right: E/R flip by Source memory, E/R flip by age, encoding activity in the E/R flip ROI by age, retrieval activity in the E/R flip ROI by age. Fit line using R's loess function with 1.3 span, and standard error marked as shaded area.

Figure 6. Hippocampus BOLD activity (parameter estimates) during encoding and retrieval. Fit line using R's loess function with 1.3 span, and standard error marked as shaded area.

Figure 7. Hippocampus volume lifespan trajectories for bilateral hippocampi. Fit line using R's loess function with 1.3 span, and standard error marked as shaded area.

Figure 8. Comparison of different approaches used for defining the E/R flip. Top left: ER/Flip ROI defined using the DM contrast, young adult sample. Middle left: E/R flip ROI defined using the baseline contrast, young adult sample (ROI used in the main analyses). Top Right: Scatterplot showing individual data points extracted from the E/R flip ROI defined using the DM approach. The black line is fitted to the E/R flip defined using the DM approach, while the green lines posted for reference represents the E/R flip defined using the baseline approach. Lines are fitted using R (ggplot2, loess span = 1.3). Bottom row: E/R flip ROI defined using different samples. Bottom left: Complete development sample, 6-30 years, n = 105. Bottom right: Complete lifespan sample, 6-80 years, n = 270.

Figure 9. Multiple comparisons corrected results showing clusters with a significant source memory - CT relation (top), and source memory age interactions (bottom). Analyses are based on the developmental subsample with complete multimodal data.

Figure 10. TFCE-corrected ($p < .05$) results showing voxels where the source memory - MD relationship differs with age. Effects are filled for readability using tbss_fill. Analyses based on the developmental subsample with complete multimodal data.

Figure 11. Scatterplots showing the data entered in the SEM model for source memory development from 6 to 30 years. Left to right: Source memory, E/R flip, MD and CT. Lines are fitted to the data using R's loess function with 1.3 span, and standard error displayed as shaded area.

Figure 12. Structural equation models. A: Initial model, B: Final model, C: Final model with encoding and retrieval entered separately. Numbers on paths represent standardized partial regression weights. Analyses are based on the developmental subsample with complete multimodal data.

Tables

Table 1: FIX performance

Threshold	1	2	**5**	10	20	30	40	50
True positive (signal)	98,5	98,5	**97**	95,6	94,2	90,7	88,9	87,8
True negative (noise)	39,3	47,6	**57,3**	66,5	75,6	79,4	82,8	87,6

Table 1. Classification accuracy over a range of thresholds, tested using the training set consisting of 16 participants. The chosen threshold 5 is shown in bold.

Table 2: Demographics and behaviour performance

	Sample		
	Development	Aging	Total
N (female/male)	105 (61/44)	165 (106/59)	270 (167/103)
Mean age (range)	19.4 (6.8–30.4)	55.8 (30.8–80.8)	41.66 (6.8-80.8)
Source Memory	53.2 % (16.4)	49.7 % (13.8)	51.1 % (14.9)
Recognition	75.7 % (11.1)	74.1 % (10.6)	74.7 % (10.8)
Misses	21.3 % (10.7)	22.4 % (10.2)	21.7 % (10.4)
False Alarms	4.5 % (5.8)	6.4 % (4.5)	5.7 % (5.1)
d' (d-prime)	2.58 (0.61)	2.27 (0.52)	2.39 (0.57)

Table 2. Demographics and memory performance scores for the development sample (left), the aging sample (middle), and the total sample (right). Range is shown for age, while the standard deviation is shown in the parentheses for the memory performance measures. The d-prime measure was derived from recognition and false alarms.

Table 3: Correlation matrix

	Sex	Age	Src mem	d-prime	E/R flip	MD	CT
Sex	1						
Age	-.026	1					
Src mem	.064	**.328**	1				
d-prime	.120	.106	**.573**	1			
E/R flip	-.077	.207	**.296**	**.409**	1		
MD	.088	-.153	-.097	-.141	-.172	1	
CT	-.113	**-.446**	**-.262**	-.018	**-.219**	.129	1
Motion	-.095	**-.599**	**-.435**	**-.234**	**-.222**	**-.344**	**-.331**

Table 3. Pearson correlation matrix. Variables from top to bottom: Sex: female = 1, male = 2; Age; Source memory; recognition d-prime; PMC E/R flip; Corrected MD; CT. Significant correlations marked in bold ($p < .05$). Data from the developmental subsample with complete multi-modal data (n=90, 6-30 years).

Table 4: Partial correlations

Bk	A-C	A−C · Bk	A−C · B∈!k	Shared %	Unique %
FLIP	0.33	0.29	0.24	**24.5 %**	**8.1 %**
MD	0.33	0.32	0.22	**6.0 %**	**0.4 %**
CT	0.33	0.24	0.28	**44.7 %**	**28.9 %**
All brain markers (B∈k)	0.33	0.22		**55.0 %**	

Table 4. Correlations and partial correlations between age (A), Source memory (C), and brain markers Bk where B∈k is the set of all brain markers (E/R flip, MD and CT), and B∈!k is all brain markers excluding the kth marker. Shared % is the percentage of variance in the age – source memory relationship that is shared with the brain marker. Unique % is the percentage of variance in the age – source memory relationship that is uniquely accounted for when all other brain markers have been partialled out.

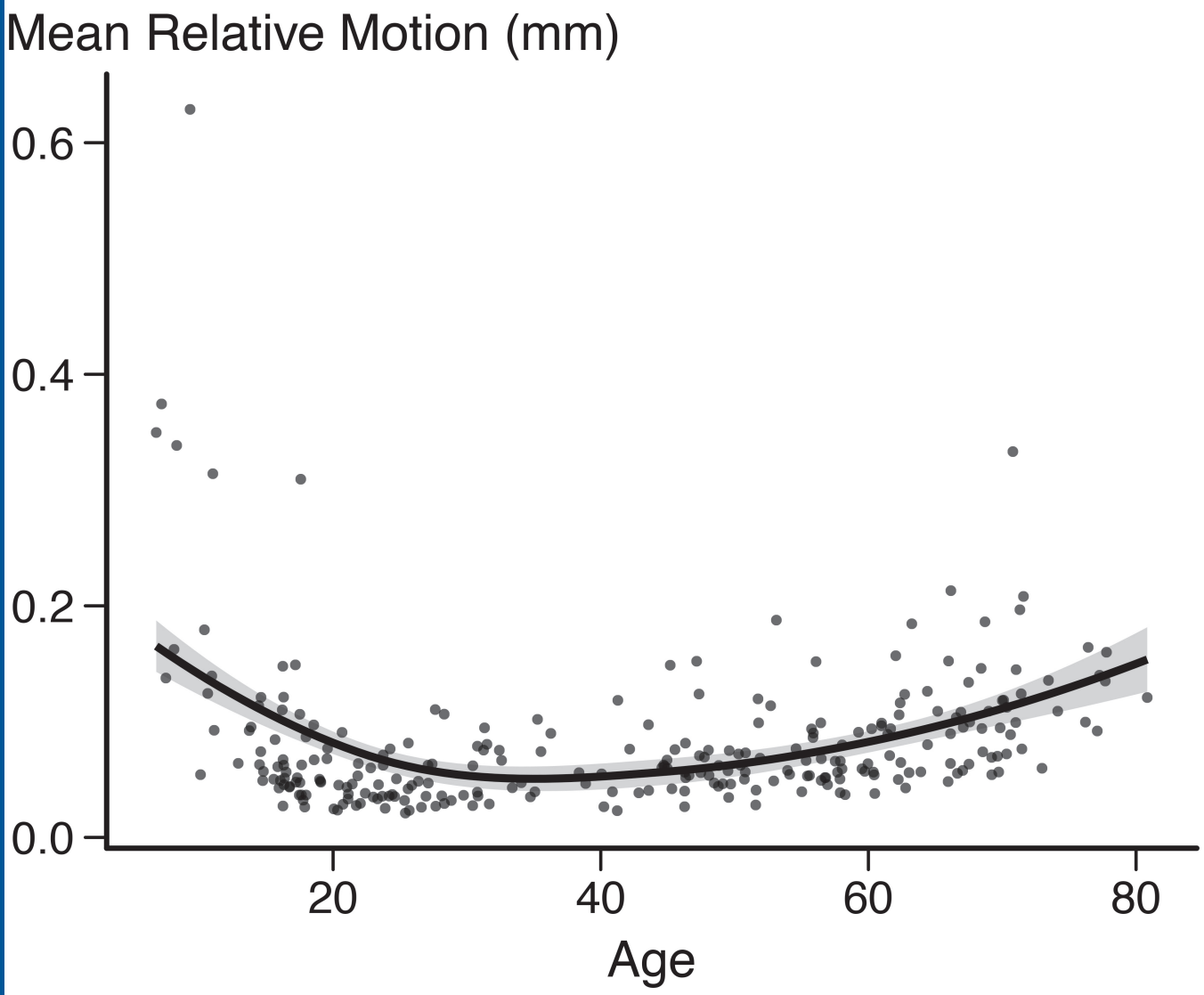

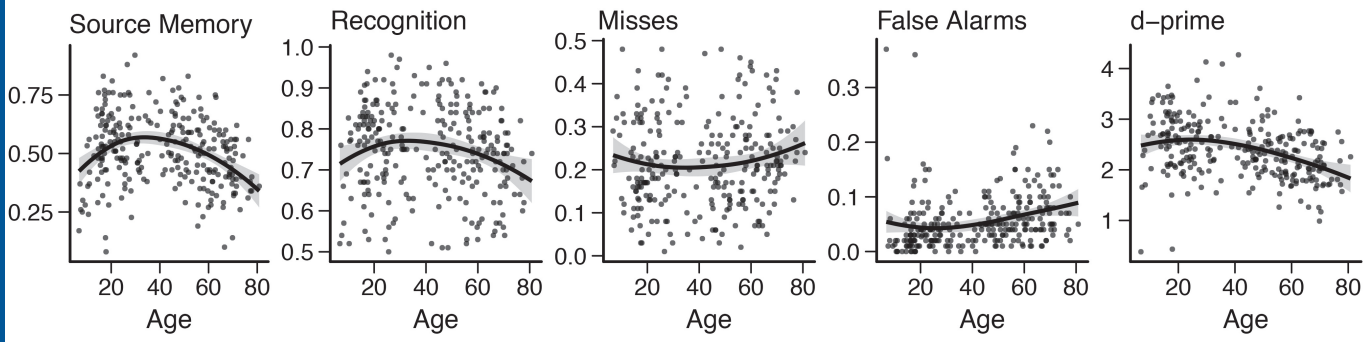

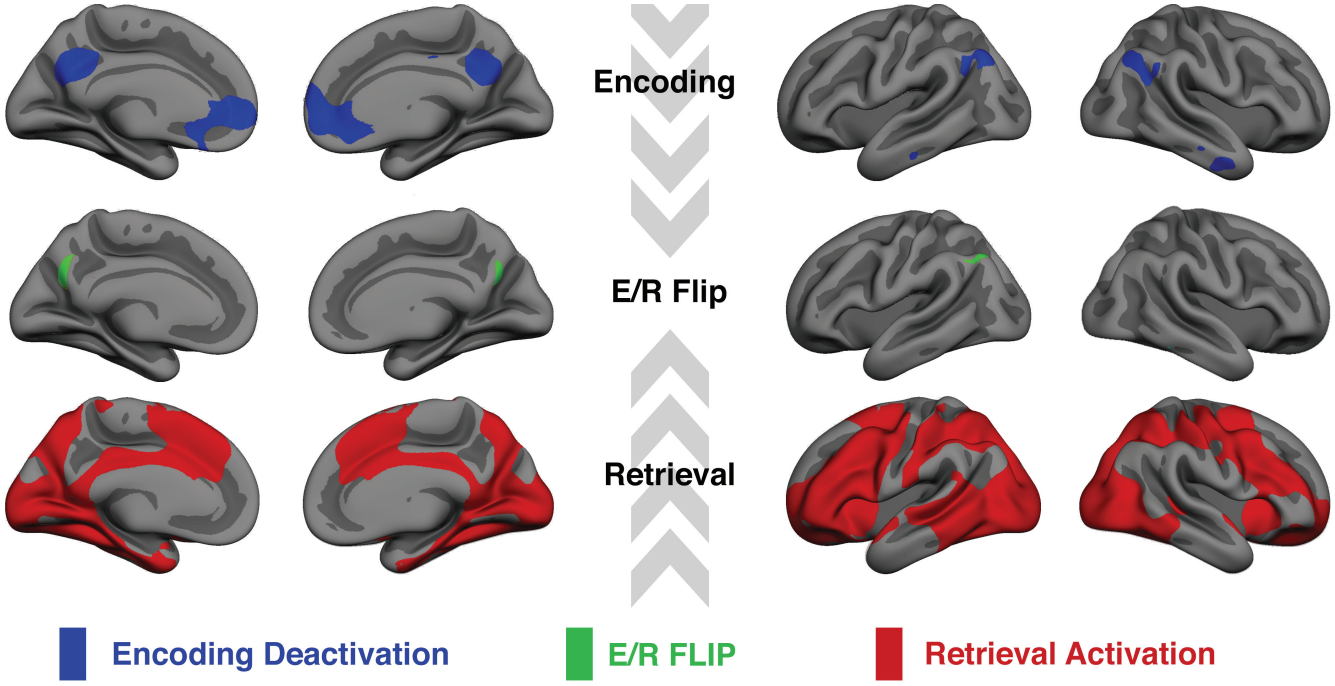

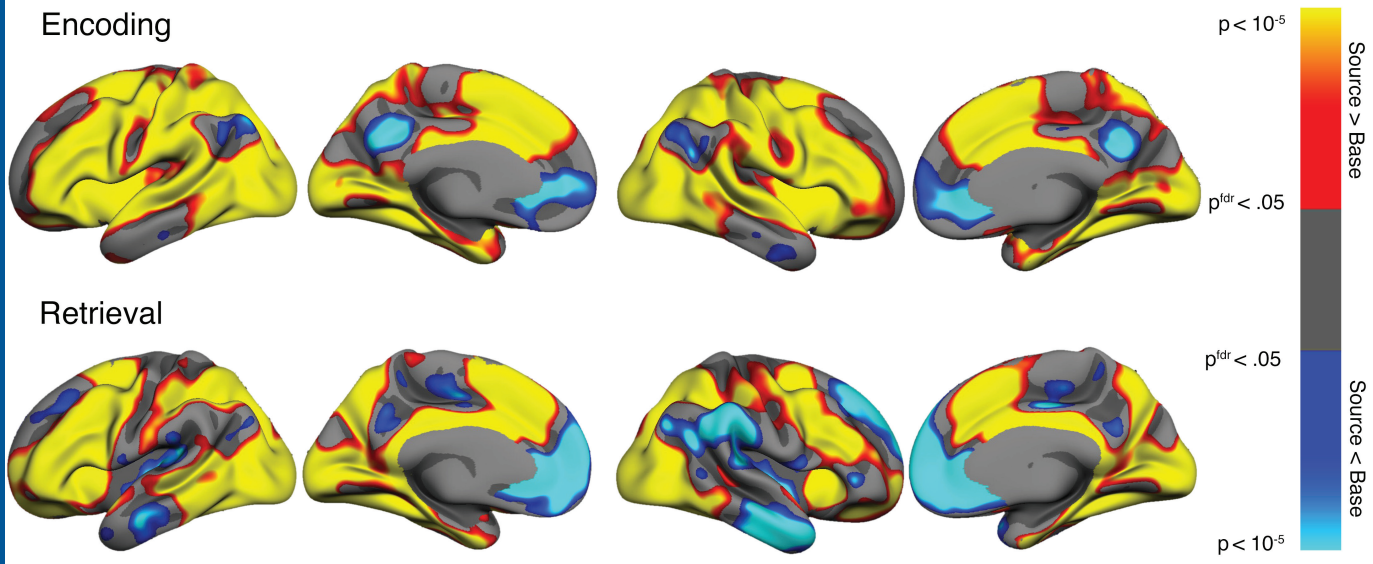

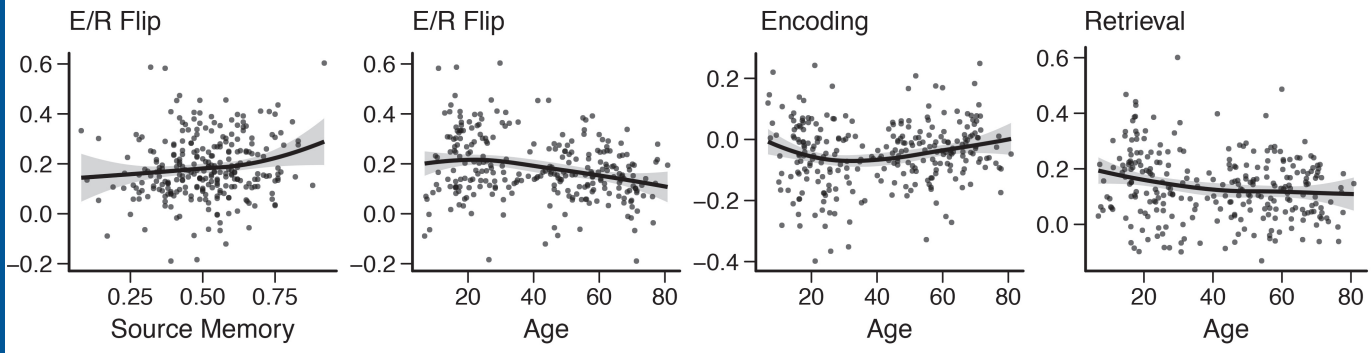

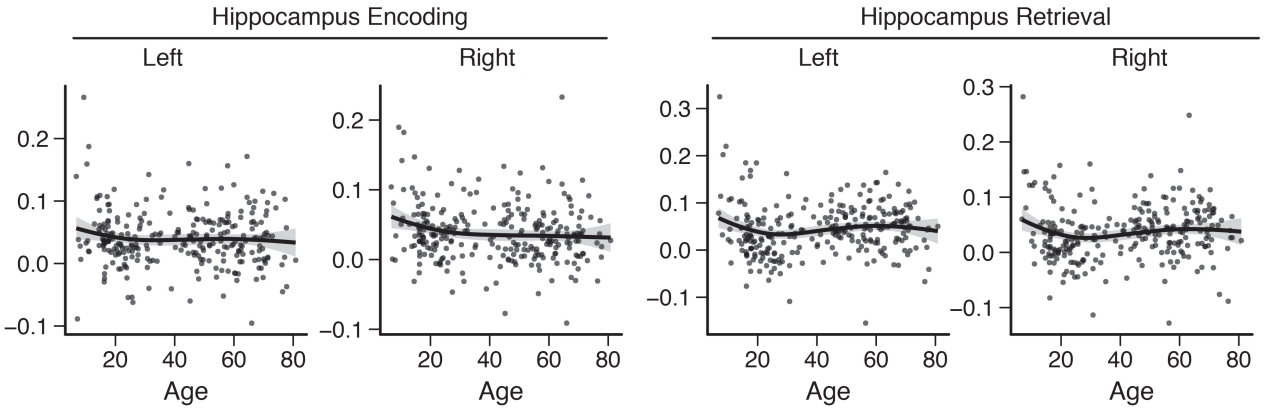

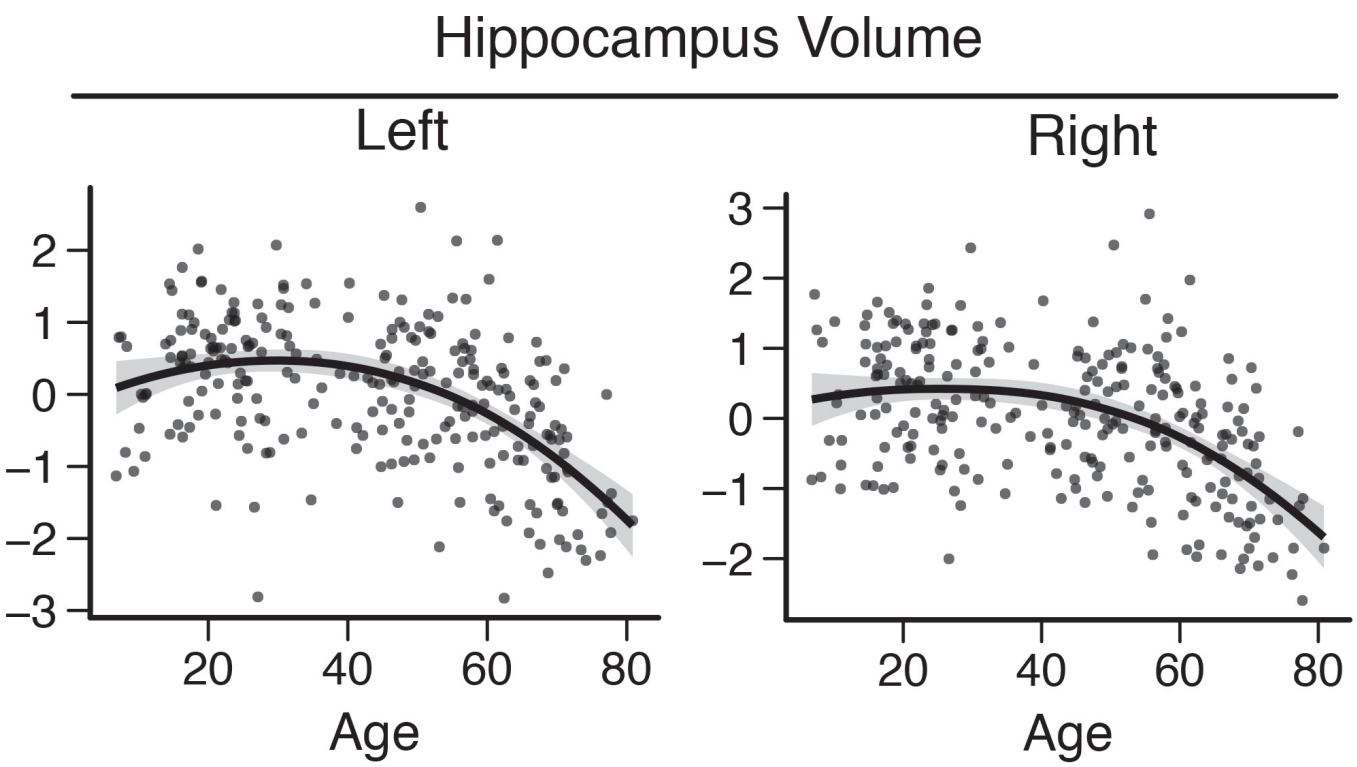

Source Memory vs. Miss
18-30 years, n = 55

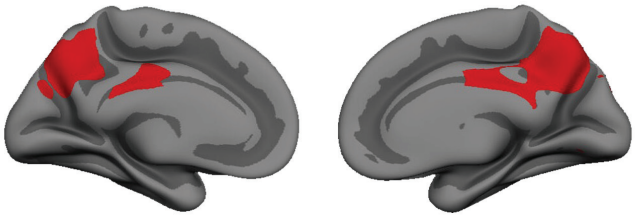

E/R FLip

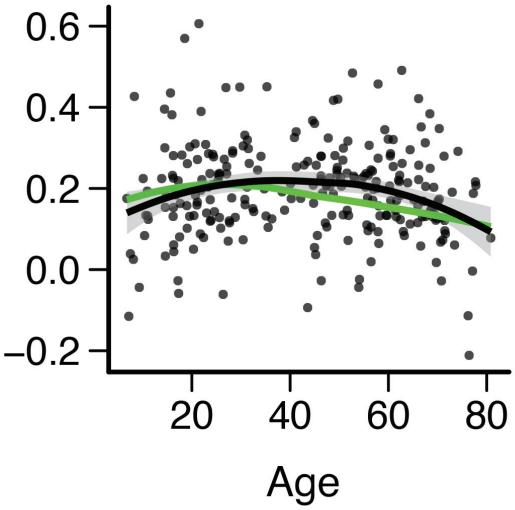

Source Memory vs. Baseline
18-30 years, n = 55

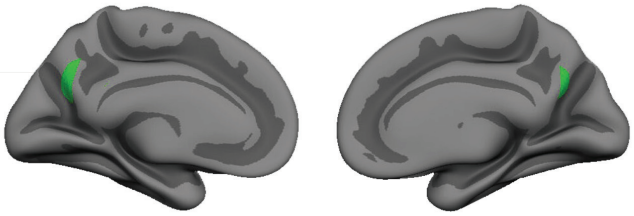

Source Memory vs. Baseline
6-30 years, n = 115

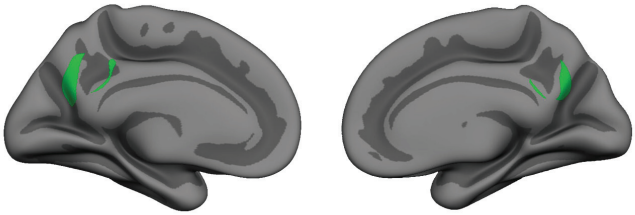

Source Memory vs. Baseline
6-80 years, n = 270

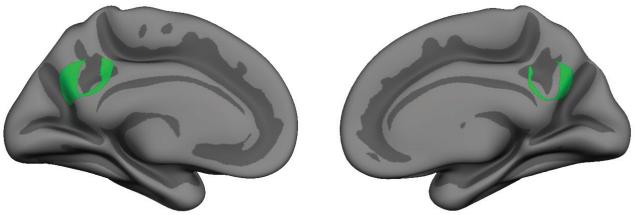

Source Memory x Age (CT)

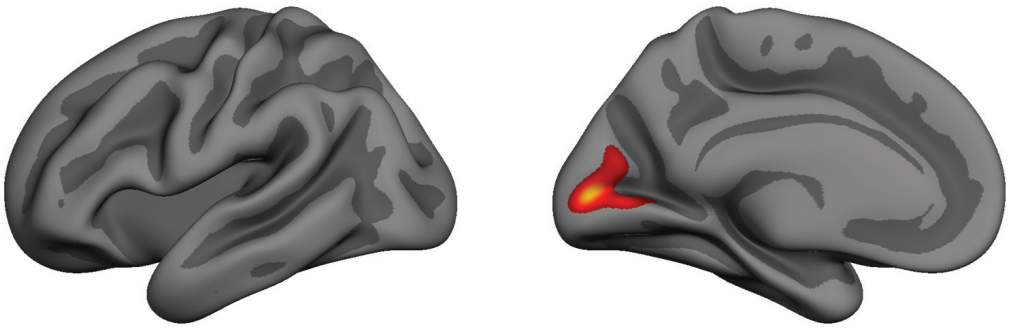

Source Memory (CT)